Int. J. Heat Mass Transfer. Vol. 31, No. 3, pp. 625–636, 1988
Printed in Great Britain

0017–9310/88 $3.00 + 0.00
Pergamon Press plc

Laminar flow heat transfer in a semi-circular tube with uniform wall temperature

R. M. MANGLIK and A. E. BERGLES
Heat Transfer Laboratory, Rensselaer Polytechnic Institute, Troy, NY 12180-3590, U.S.A.

(*Received* 27 *April* 1987 *and in final form* 10 *July* 1987)

Abstract—Constant property, laminar flow heat transfer in a semi-circular tube with uniform wall temperature has been analyzed. The results define the lower bound of heat transfer augmentation in circular tubes with twisted-strip inserts. Two thermal boundary conditions, corresponding to two extremes of the fin effect of the inserts encountered in practical applications, are considered. Numerical solutions employing finite-difference formulations have been carried out. For a hydrodynamically fully developed flow, the friction factor of $(15.823/Re)_{D_h}$ agrees with the analytical solution reported in the literature. Results for thermally developing flow heat transfer are presented graphically, and equations (28) and (29) describe the solutions for Nu_m as a function of Gz for the two boundary conditions. The asymptotic Nusselt numbers for the two cases are 5.626 and 4.631.

INTRODUCTION

TWISTED-STRIP inserts are a particularly effective technique for enhancing laminar flow heat transfer in circular tubes [1]. The swirl flow effects diminish as the severity of the twist is decreased. In the limit, the strip is straight and the tube is divided into two circular segment ducts. When the strip is thin, the situation is essentially that of flow in a semi-circular duct. A solution for the heat transfer in laminar flow in a semi-circular tube would, therefore, provide the necessary limiting base-line reference for the more general enhancement problem with twisted-strip inserts in circular tubes.

Shah and London [2] have extensively surveyed laminar flows in ducts of different geometries. Laminar flow with heat transfer in ducts of circular segment and semi-circular cross-sections was first analyzed by Eckert *et al.* [3] and Sparrow and Haji-Sheikh [4]. They presented isothermal friction factors and Nusselt numbers for fully developed flows with the uniform heat flux boundary condition. Hong and Bergles [5] considered the hydrodynamically developed, but thermally developing, laminar flow problem in a semi-circular tube. Their numerical solutions for the thermal entrance region treat two variations of the uniform axial heat rate boundary condition: uniform peripheral wall temperature at each axial location, and uniform wall temperature around the semi-circular arc but zero heat flux along the straight section. These solutions simulate an electrically heated tube with large peripheral thermal conductors where the strip insert is, respectively, a good conductor and in excellent contact with the wall or a poor conductor in poor contact with the wall.

For process industry applications, it is more usual to encounter the uniform wall temperature boundary condition commonly produced by steam heating. For this case, however, there does not appear to be a heat transfer solution described in the literature. It is the intent in this paper to analyze this problem and present numerical solutions for both the thermal entrance region and fully developed flow. The analysis accounts for two boundary conditions, namely, uniform wall temperature peripherally and axially, and uniform wall temperature peripherally and axially over the circular section but with the straight section adiabatic. These two conditions essentially form the lower extremes of the fin effect of a twisted-strip insert. The former signifies that the twisted strip is a perfect heat conductor and is in perfect thermal contact with the tube, while the latter condition considers the strip to be insulated from the wall, or a heat nonconductor. In actual practice, a loose-fitting metallic strip of relatively low thermal conductivity is usually employed, which corresponds to a situation in between these two boundary conditions.

PROBLEM FORMULATION

Thermal entrance region

The basic analysis involves the cylindrical coordinate system (R, θ, Z), shown in Fig. 1(a). The steady, incompressible, laminar flow is considered to be hydrodynamically fully developed but thermally developing. From boundary layer theory, this idealization appears to be valid for most liquids with high Prandtl numbers ($Pr \gg 1$) where the hydrodynamic entry length is relatively very small [6]. Additionally, the problem formulation is constrained by the following simplifications:

(1) Newtonian fluid, constant property flow;
(2) constant axial pressure gradient;
(3) negligible axial heat conduction;
(4) negligible viscous dissipation.

NOMENCLATURE

a	inner radius of semi-circular tube
C	dimensionless pressure drop parameter, $(a^2/\mu\bar{W})(\partial P/\partial Z)$
C_1	a constant, $2(\pi+2)/\pi$ for Case 1, and 2 for Case 2
C_p	specific heat
D_h	hydraulic diameter, equation (6)
f	Fanning friction factor
G	a function, $(w\phi\, Nu\, C_1)/2$
Gz	Graetz number, $\dot{m}C_p/kL$
g	dimensionless parameter, w/C
h	heat transfer coefficient, equation (9)
i	radial grid point
j	circumferential grid point
k	thermal conductivity; axial grid point
L	axial length of duct
M	radial mesh size
$\dot{m}$	mass flow rate
N	circumferential mesh size; normal coordinate
n	dimensionless normal coordinate, N/a
Nu	Nusselt number, $2ah/k$
Nu_m	axially mean Nusselt number, equation (14)
P	pressure
Pe	Peclet number, $Re\,Pr$
Pr	Prandtl number, $\mu C_p/k$
q''_w	local peripherally averaged wall heat flux
R	radial component of cylindrical coordinate system
Re	Reynolds number, $\rho\bar{W}D/\mu$
Re_a	Reynolds number based on radius, $\rho\bar{W}a/\mu$
Re_{D_h}	Reynolds number based on hydraulic diameter, $\rho\bar{W}D_h/\mu$
r	dimensionless radial coordinate, R/a
T	temperature
T_m	bulk fluid temperature
T_i	fluid temperature at duct inlet
UHF	uniform heat flux
UWT	uniform wall temperature
W	axial velocity
$\bar{W}$	average axial velocity, equation (21)
w	dimensionless axial velocity, $W/\bar{W}$
Z	axial component of cylindrical coordinate system
z	dimensionless axial coordinate, $Z/a(Re_a\,Pr)$.

Greek symbols

θ	circumferential component of cylindrical coordinate system
μ	fluid viscosity
ρ	fluid density
τ_w	shear stress at duct wall, equations (3) and (4)
ϕ	dimensionless temperature, $(T_w-T)/(T_w-T_i)$
ϕ_m	dimensionless bulk temperature, $(T_w-T_m)/(T_w-T_i)$.

Subscripts

i	at a radial node point
i,j	at a grid point in duct cross-section
i,j,k	at a grid point in flow field
j	at a circumferential node point
k	at an axial grid point
m	mean
w	at duct wall.

The consideration of these assumptions does not necessarily imply an oversimplification of the problem. Singh [7] established that axial heat conduction effects are negligible in flows with Peclet number ($Re\,Pr$) greater than 100. Collins [8] observed that viscous dissipation effects are negligible and need not be included in most laminar flow analyses. The only major idealization, therefore, is the assumption of constant properties. In real situations, as pointed out in refs. [9, 10], experimental heat transfer data exhibit substantial deviations from constant property analytical predictions. This is attributable to the temperature dependence of transport and thermophysical properties of fluids. Nevertheless, as stipulated earlier, the chief objective here is to arrive at a limiting solution, and to this end a constant property analysis is a good approximation. Furthermore, as noted earlier, the thermal analysis is constrained by either of the two boundary conditions given below.

Case 1: uniform axial and circumferential tube wall temperature.

Case 2: adiabatic straight section but constant axial and circular arc section tube wall temperature.

These two conditions are schematically illustrated in Fig. 1(b).

In order to render the requisite governing equations dimensionless, the following parameters are defined:

$$Re_a = \frac{\rho\bar{W}a}{\mu}, \quad Pr = \frac{\mu C_p}{k}, \quad r = \frac{R}{a}, \quad w = \frac{W}{\bar{W}}$$

$$z = \frac{Z}{a\,Re_a\,Pr}, \quad \phi = \frac{T_w-T}{T_w-T_i}, \quad C = \frac{a^2}{\mu\bar{W}}\frac{\partial P}{\partial Z}.$$

With the introduction of these parameters and the assumptions in the problem statement, the governing differential equations can be expressed in dimensionless form as [11]:

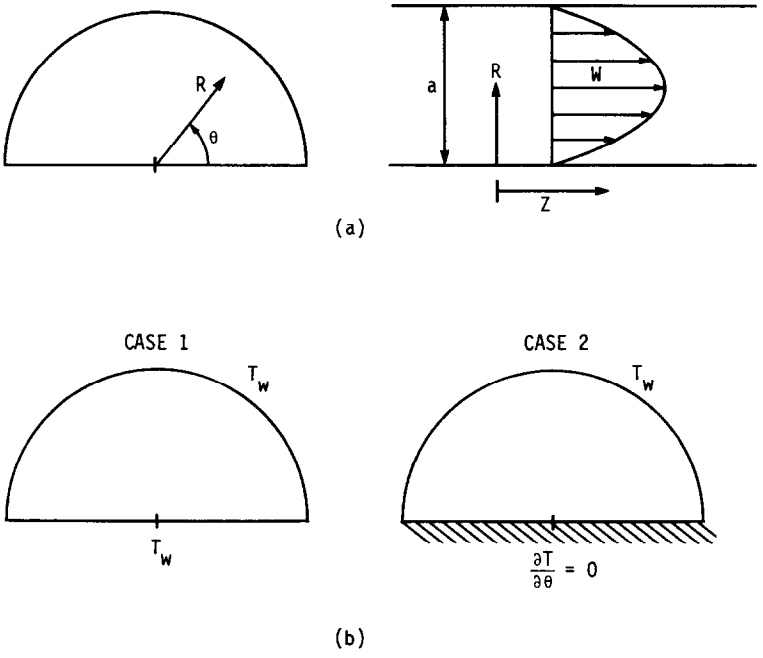

FIG. 1. Flow field configurations: (a) coordinate system with velocity profile; (b) thermal boundary conditions.

momentum equation

$$\frac{\partial^2 w}{\partial r^2} + \frac{1}{r}\frac{\partial w}{\partial r} + \frac{1}{r^2}\frac{\partial^2 w}{\partial \theta^2} = C; \tag{1}$$

energy equation

$$\frac{\partial^2 \phi}{\partial r^2} + \frac{1}{r}\frac{\partial \phi}{\partial r} + \frac{1}{r^2}\frac{\partial^2 \phi}{\partial \theta^2} = w\frac{\partial \phi}{\partial z}. \tag{2}$$

The boundary conditions for these equations, in terms of dimensionless parameters, are:

for the momentum equation

$$w(1,\theta) = 0$$

$$w(r,\theta) = 0 \quad \text{at} \quad \theta = 0 \text{ and } \pi;$$

for the energy equation

$$\phi(r,\theta,0) = 1$$

$$\phi(1,\theta,z) = 0, \quad 0 < \theta < \pi$$

Case 1: $\phi(r,\theta,z) = 0$ at $\theta = 0$ and π

Case 2: $(\mathrm{d}\phi/\mathrm{d}\theta) = 0$ at $\theta = 0$ and π; $0 < r < 1$.

The solution of these equations yields the velocity and temperature fields which, in turn, provide the friction factor and Nusselt number.

Friction factor

To evaluate the friction factor, a stationary control volume in the flow field is considered from which the following expression for the wall shear stress is obtained

$$\tau_w = -\frac{a}{2}\left(\frac{\pi}{\pi+2}\right)\left(\frac{\mathrm{d}P}{\mathrm{d}Z}\right). \tag{3}$$

However, by definition of the friction factor

$$\tau_w = f \cdot \tfrac{1}{2}\rho \bar{W}^2 \tag{4}$$

and a hydraulic diameter based Reynolds number is given by

$$Re_{D_h} = \frac{\rho D_h \bar{W}}{\mu} \tag{5}$$

where

$$D_h = 2a\left(\frac{\pi}{\pi+2}\right). \tag{6}$$

Therefore, by combining equations (3)–(6) and introducing the dimensionless pressure drop constant, C, the friction factor is given by

$$(f\,Re)_{D_h} = -2C\left(\frac{\pi}{\pi+2}\right)^2. \tag{7}$$

Equations (1) and (7) can be readily solved for w and $(f\,Re)$ by a numerical iterative procedure.

Nusselt number

The heat transfer result of primary thermal design importance is the coefficient of heat transfer. The usual expression for the Nusselt number is

$$Nu = \frac{2ah}{k}. \tag{8}$$

The peripherally averaged, but axially local, heat transfer coefficient, h, is generally defined by

$$\dot{q}''_w = h(T_w - T_m). \tag{9}$$

Introducing a dimensionless mixed-mean fluid temperature

$$\phi_m = \frac{T_w - T_m}{T_w - T_i} \tag{10}$$

and the non-dimensional equation for the heat flux at the duct wall

$$\dot{q}''_w = \frac{k(T_w - T_i)}{a}\left(\overline{\frac{\partial\phi}{\partial n}}\right)_w \tag{11}$$

into equation (9) and combining it with equation (8) yields

$$Nu = -\frac{2}{\phi_m}\left(\overline{\frac{\partial\phi}{\partial n}}\right)_w \tag{12}$$

where $(\overline{\partial\phi/\partial n})_w$ represents a peripheral average temperature gradient at the duct wall. The dimensionless mixed-mean temperature, given the local velocity and temperature fields, is evaluated from

$$\phi_m = \frac{2}{\pi}\int_0^1 \int_0^\pi w\phi r \, d\theta \, dr. \tag{13}$$

The Nusselt number given by equation (12) is the axially local, but peripherally mean value. In process heat exchanger design and rating a mean axial Nusselt number, rather than a local one, has greater functional applicability. This is represented by a mean heat transfer coefficient averaged over the tube length

$$Nu_m = \frac{1}{z}\int_0^z Nu \, dz. \tag{14}$$

Thus, with the solution of the energy equation (2), ϕ_m, Nu, and Nu_m can be numerically evaluated from equations (13), (12), and (14), respectively. This arithmetic can be conveniently repeated for the two thermal boundary conditions to complete the heat transfer solution for laminar, constant property flow in a semicircular tube.

Fully developed flow

The attainment of fully developed velocity and temperature profiles is usually considered to be fully developed flow. For a given heating rate, it is reasonable to assume that at axial locations far removed from the duct entrance, the temperature profile will be fully established and will not exhibit any variation [6]. The fact that the temperature profile is invariant with axial distance Z can be stated mathematically in its dimensionless form as

$$\frac{\partial\phi}{\partial z} = \frac{\phi}{\phi_m}\frac{d\phi_m}{dz}. \tag{15}$$

Next, from an energy balance over an elemental duct segment of length dZ, it can be shown that

$$\frac{d\phi_m}{dz} = \frac{C_1}{2}\phi_m Nu \tag{16}$$

where C_1 is evaluated according to Case 1 and Case 2 thermal boundary conditions as follows:

$$C_1 = 2(\pi+2)/\pi \quad \text{for Case 1}$$

$$C_1 = 2 \quad \text{for Case 2.}$$

Hence, with the substitution of equations (15) and (16), the energy equation (2) can be transformed for the fully developed flow condition to

$$\frac{\partial^2\phi}{\partial r^2} + \frac{1}{r}\frac{\partial\phi}{\partial r} + \frac{1}{r^2}\frac{\partial^2\phi}{\partial\theta^2} = \frac{C_1}{2}w\phi Nu. \tag{17}$$

The thermal boundary constraints are the same as stated earlier for equation (2).

FINITE-DIFFERENCE FORMULATION

Numerical solutions for laminar flows with heat transfer in ducts of various cross-section geometries have been widely reported in the literature. The numerical analysis strategies adopted here are essentially based on the recommendations of Hornbeck [12]. For the flow field configuration described by the coordinate system of Fig. 1(a), the finite-difference grid used is shown in Fig. 2. The mesh is equally spaced in the radial (r) and circumferential (θ) directions, but not in the axial (z) direction. The axial node points are denoted by k, and the grid points in the r- and θ-directions by i and j, respectively.

Fully developed velocity solution

The momentum equation as described by equation (1) has two unknowns: the axial velocity, w, and the pressure drop constant, C. However, with the substitution of the parameter g defined as

$$g = \frac{w}{C} \tag{18}$$

equation (1) reduces to

$$\frac{\partial^2 g}{\partial r^2} + \frac{1}{r}\frac{\partial g}{\partial r} + \frac{1}{r^2}\frac{\partial^2 g}{\partial\theta^2} = 1. \tag{19}$$

The corresponding no-slip boundary conditions in terms of g can be stated as

$$g(1,\theta) = 0$$

$$g(r,\theta) = 0 \quad \text{at} \quad \theta = 0 \text{ and } \pi.$$

The finite-difference representation for the grid as shown in Fig. 2, can be expressed as

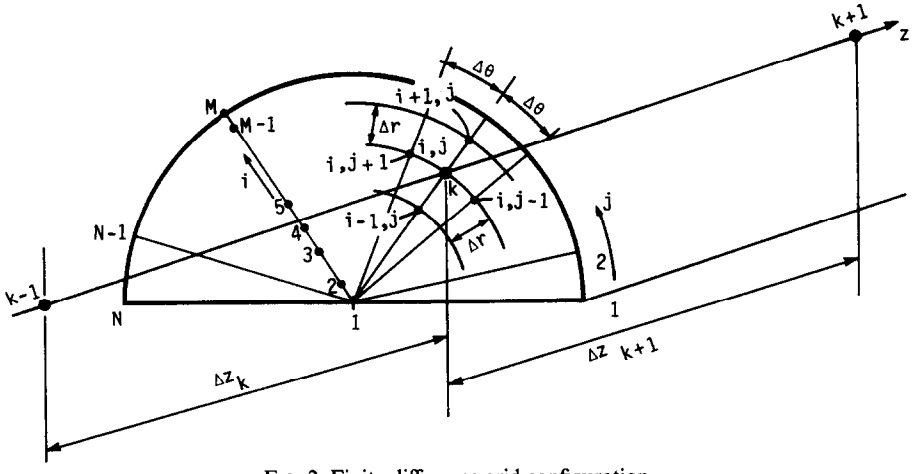

FIG. 2. Finite-difference grid configuration.

$$\frac{1}{\Delta r}\left[r_{i+1/2}\cdot\frac{g_{i+1,j}-g_{i,j}}{\Delta r}-r_{i-1/2}\cdot\frac{g_{i,j}-g_{i-1,j}}{\Delta r}\right]+\frac{1}{r_i}\left[\frac{g_{i,j+1}-2g_{i,j}+g_{i,j-1}}{(\Delta\theta)^2}\right]=r_i. \quad (20)$$

This is an explicit representation with the only unknown at the (i, j) node point, and its solution can be effected through a simple relaxation technique [11]. To calculate the pressure drop constant, C, the usual definition of the average velocity, $\bar{W}$, given by

$$\bar{W}=\frac{1}{A_c}\int_{A_c}W\,\mathrm{d}A_c=\frac{2}{\pi a^2}\int_0^a\int_0^\pi WR\,\mathrm{d}\theta\,\mathrm{d}R \quad (21)$$

is introduced in equation (18) to obtain

$$C=\frac{\pi}{2\iint gr\,\mathrm{d}\theta\,\mathrm{d}r}. \quad (22)$$

This can be numerically integrated by employing the trapezoidal rule. Finally, knowing g and C, the axial velocity distribution is determined from equation (18).

Thermal entrance region

Using an implicit scheme, the finite-difference representation of a rephrased form of the energy equation (2) [11] is

$$-\left[r_i\left(r_i-\frac{\Delta r}{2}\right)(\Delta\theta)^2\Delta z\right]\phi_{i-1,j,k}+\left[(r_i\Delta r\Delta\theta)^2w_{i,j}+2(r_i\Delta\theta)^2\Delta z+2(\Delta r)^2\Delta z\right]\phi_{i,j,k}-\left[r_i\left(r_i+\frac{\Delta r}{2}\right)(\Delta\theta)^2\Delta z\right]\phi_{i+1,j,k}$$
$$=(r_i\Delta r\Delta\theta)^2w_{i,j}\phi_{i,j,k-1}+\Delta z(\Delta r)^2\left[\phi_{i,j+1,k}+\phi_{i,j-1,k}\right]. \quad (23)$$

With the imposition of the given boundary conditions, the matrix of the coefficients of the set of linear algebraic equations that are generated is tridiagonal and can be solved by the Thomas algorithm [13]. The temperature field is solved separately for both Case 1 and Case 2 boundary conditions. The details of the finite-difference formulations corresponding to the application of the boundary constraints along with the consequent series of algebraic equations are given in ref. [11].

Once the local temperature distribution is established, the bulk temperature, θ_m, is directly obtainable from equation (13) by a simple numerical integration employing the trapezoidal rule. Furthermore, the circumferentially averaged temperature gradient at the wall at a given z location can be numerically determined from

$$\left(\frac{\overline{\partial\phi}}{\partial n}\right)_w=\frac{1}{(\pi+2)}\times\left[\frac{\pi}{(N-2)}\sum_{j=2}^{N-1}\left(\frac{3\phi_{M,j}-4\phi_{M-1,j}+\phi_{M-2,j}}{2\Delta r}\right)+\frac{2}{(2M-3)}\left\{\sum_{i=2}^{M-1}\left(\frac{3\phi_{i,1}-4\phi_{i,2}+\phi_{1,3}}{2r_i\Delta\theta}\right)+\sum_{i=2}^{M-1}\left(\frac{3\phi_{i,N}-4\phi_{i,N-1}+\phi_{i,N-2}}{2r_i\Delta\theta}\right)+\left(\frac{3\phi_{1,1+N/2}-4\phi_{2,1+N/2}+\phi_{3,1+N/2}}{2\Delta r}\right)\right\}\right]. \quad (24)$$

Equation (24) is only applicable for the Case 1 boundary condition where the wall temperature is specified,

i.e. $\theta = 0$. For the Case 2 boundary condition, where the flat section is considered to be adiabatic, equation (24) reduces to

$$\left(\frac{\partial\phi}{\partial n}\right)_w = \frac{1}{(N-2)}\sum_{j=2}^{N-1}\left(\frac{3\phi_{M,j}-4\phi_{M-1,j}+\phi_{M-1,j}}{2\Delta r}\right). \quad (25)$$

Thus, the axially local Nusselt number can be determined by evaluating equations (13), (24), (25), and (12) for the two boundary conditions. The mean Nusselt number is obtainable by numerically integrating equation (14) using the trapezoidal rule.

Fully developed flow

The fully developed flow solution provides the necessary asymptotic result for a complete analysis of the heat transfer problem. The separate solution of this condition is driven by the need to obtain an independent verification of and to establish an unequivocal result for the asymptotic Nusselt number in constant property, laminar flows in semi-circular tubes with UWT.

The energy equation governing the fully developed flow is elliptic in nature and has two unknowns: the dimensionless temperature, θ, and the Nusselt number (which is a function of θ). By introducing a parameter G, defined as

$$G_{i,j} = \frac{C_1}{2} w_{i,j}\phi_{i,j} Nu \quad (26)$$

equation (17) can be restated [11] to give the following finite-difference representation:

$$-\left[r_i\left(r_i-\frac{\Delta r}{2}\right)(\Delta\theta)^2\right]\phi_{i-1,j}+2\left[(r\Delta\theta)^2+(\Delta r)^2\right]\phi_{i,j}$$
$$-\left[r_i\left(r_i+\frac{\Delta r}{2}\right)(\Delta\theta)^2\right]\phi_{i+1,j} =$$
$$(\Delta r)^2(\phi_{i,j+1}+\phi_{i,j-1})-(r_i\Delta\theta\Delta r)^2 G_{i,j}. \quad (27)$$

Here again, a set of linear algebraic equations will be obtained and the coefficient matrix is tridiagonal for both Case 1 and Case 2 boundary conditions. The solution for θ and Nu can be obtained through a series of iterative steps involving equations (26), (27), (13), (24), (25), and (12) as described in detail in ref. [11].

NUMERICAL SOLUTION METHOD

The numerical literature generally acknowledges that consistent and stable initial value problems are convergent. The finite-difference schemes adopted in this study, with truncation errors of the order of the square of the mesh size, are consistent and universally stable. However, as recently documented by Conley *et al.* [14], most numerical solutions to the Graetz problem deviate from the exact closed-form solutions in the immediate vicinity of the duct entrance. They have attributed this to what was observed by Collins [15] as a general error of about 1% that is commonly incurred in the numerical resolution of energy balances for explicitly imposed wall thermal conditions. This error is also found to be much greater near the entrance [15], caused by gross numerical approximations of the sharp axial and radial gradients in this region. Shah and London [2] ascribe the deviations to the singularity at the duct mouth where the Nusselt number is infinity and rather coarse approximations for this condition. Notwithstanding the reasons for the discrepancies, Conley *et al.* [14] have shown through a rigorous comparative numerical analysis that the selection of optimally fine radial and axial grid sizes greatly reduces the inaccuracy. What little error that might persist, in spite of a fine grid very near the duct entrance, is not of grave significance in most practical applications [2].

For the grid selection in this study, trial runs for the momentum equation and an initial part of the thermal entry length solution were conducted. Based on these results, a 41 × 41 mesh was adopted for the thermal entrance region and a 21 × 21 grid for the fully developed energy equation. For the marching solution of the energy equation, the initial axial step was fixed through a reasonably extensive trial process to be

$$\Delta z = 0.00015.$$

Furthermore, to conserve computation time and avoid unnecessary refinement downstream in the flow field, a successively increasing axial mesh was chosen. The increase in the Δz step was governed by the following equation:

$$\Delta z_i = \Delta z_{i-1} \times 1.22, \quad i = 1, 2, 3, \text{ etc.}$$

The iterative convergence criterion was established to have a maximum error of less than 0.0001. The Gauss–Seidel method with SOR was employed for the velocity solution. For the energy equations SOR by rows was used for Case 1 and under-relaxation for Case 2. Details of the solution procedures and the concomitant computer codes are given in ref. [11].

RESULTS AND DISCUSSION

Velocity solution

The fully developed axial velocity distribution at different circumferential (θ) locations in the duct cross-section is given in Fig. 3. The velocity profile has approximately a parabolic shape, particularly at $\theta = 90°$. At locations closer to the straight wall the profile tends to flatten out. The present numerical solution agrees very well with the results of Hong and Bergles [16], as shown in Fig. 3. The friction factor as given by equation (7), after the numerical integration of equation (22), was evaluated as

$$(f\,Re)_{D_h} = 15.823.$$

This is in excellent agreement with the analytical solu-

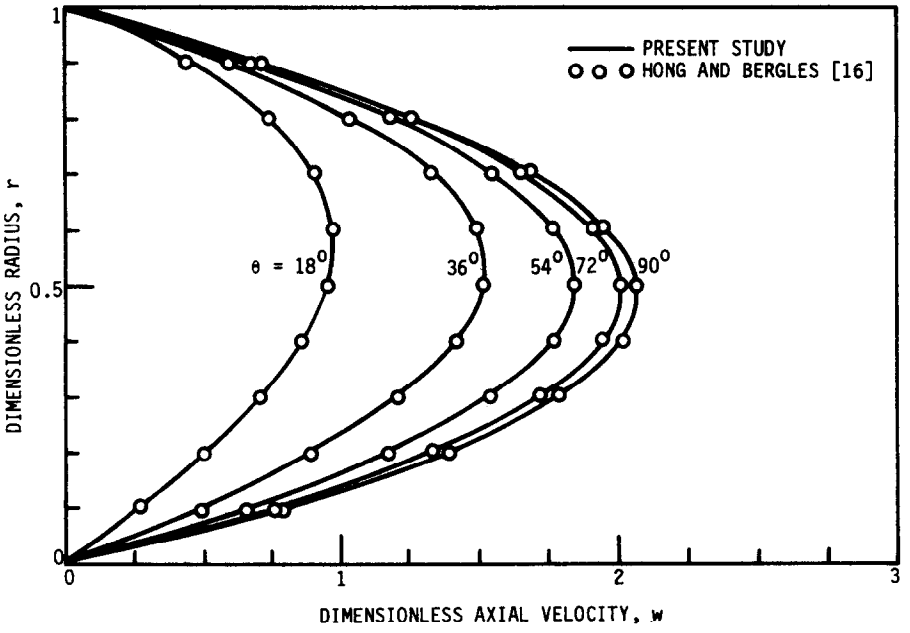

FIG. 3. Fully developed axial velocity distribution.

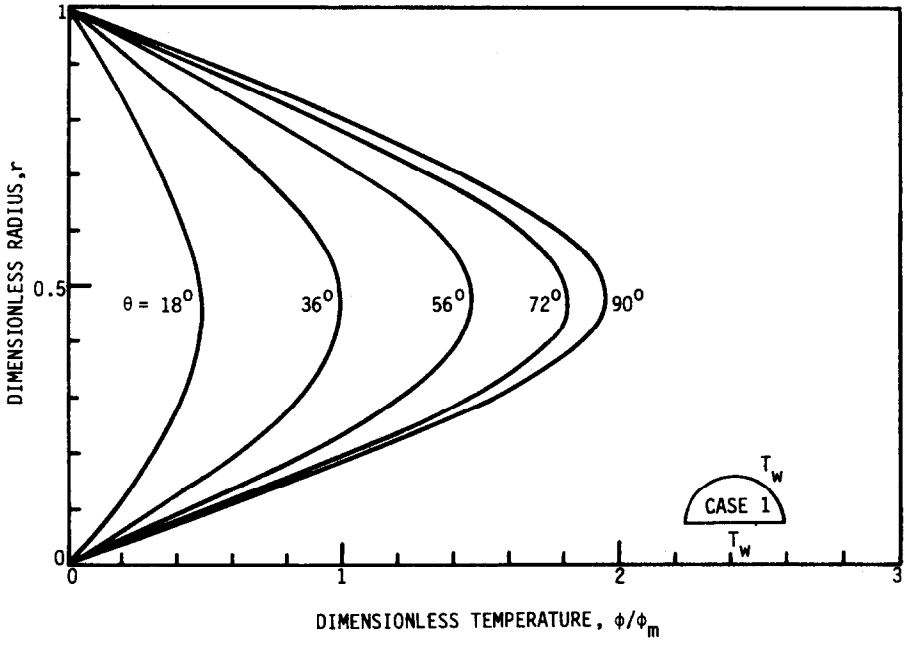

FIG. 4. Fully developed dimensionless temperature profile for Case 1 thermal boundary condition.

tion of Sparrow and Haji-Sheikh [4], who have reported $(f\,Re)_{D_h} = 15.767$. The slight deviation is probably due to the inherent approximations in a numerical solution.

Fully developed flow heat transfer

For a constant property, laminar flow in a semi-circular tube with the Case 1 boundary condition, the fully developed temperature profile is presented in Fig. 4. The profile is similar to the shape generally depicted for flows in circular tubes with UWT [2, 6], i.e. a nearly parabolic shape. Figure 5 illustrates the temperature profile for the case of an insulated straight wall section in the semi-circular tube (Case 2). Zero temperature gradients, resulting from no heat transfer from the straight wall section, are evident from the somewhat flat profile at and near $r = 0$.

The corresponding Nusselt numbers as obtained

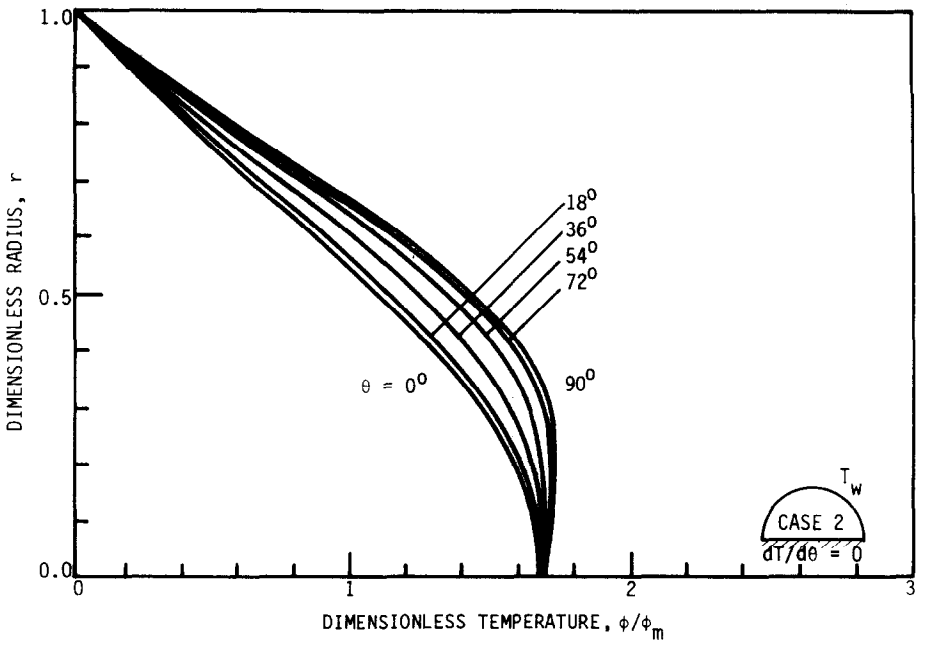

FIG. 5. Fully developed dimensionless temperature profile for Case 2 thermal boundary condition.

Table 1. Comparison of asymptotic Nusselt numbers in UWT and UHF boundary conditions

Duct geometry	Thermal boundary conditions UWT		UHF
Semi-circular	Case 1	5.626†	6.724 [5]; 6.692 [4]
	Case 2	4.631†	5.172 [5]
Circular		3.657 [2]	4.364 [2]

† Results from the present study.

for the two boundary conditions are

$$\text{Case 1}: Nu = 5.626$$
$$\text{Case 2}: Nu = 4.631.$$

As would be expected from the larger heat transfer area of Case 1, this Nusselt number is higher than that for the Case 2 boundary condition. An interesting comparison of the heat transfer coefficients for the present UWT case with the asymptotic UHF results is presented in Table 1. The circular tube Nusselt numbers for the two thermal boundary conditions are also tabulated. The UWT results are evidently lower than the corresponding UHF Nusselt numbers. This, according to Shah and London [2], results from the smaller temperature gradient at the wall in the UWT case, due to the slight inflection in the temperature profile near the wall. Nevertheless, in either situation, the heat transfer coefficients for semi-circular tubes are seen to be greater than those for circular tubes.

Thermal entrance region heat transfer

The thermal entrance region solution considered here presupposes a fully developed velocity profile as presented in Fig. 3. For the Case 1 boundary condition, the numerical marching solution of the governing energy equation resulted in the temperature profiles (at $\theta = 90°$) shown in Fig. 6. The uniform temperature profile at the duct entrance grows to a 'parabolic' profile as the fluid flows downstream and the thermal boundary layer attains the fully developed condition. A similar development of the temperature profiles (at $\theta = 90°$) in the entrance region for the Case 2 thermal boundary condition is presented in Fig. 7. The flat profiles at $r = 0$ are indicative of the adiabatic condition in the straight wall section of the semi-circular tube. As in the previous case, the temperature profile assumes a definite curvilinear shape further downstream in the flow field.

Figure 8 shows the heat transfer results for Case 1, as characterized by mean axial Nusselt numbers, Nu_m, at different Graetz numbers. The circumferentially averaged, but axially local, Nusselt numbers, Nu, and the bulk fluid temperatures, θ_m, are also plotted in Fig. 8. Similar results for the marching solution for the Case 2 thermal boundary condition are presented in Fig. 9. For design purposes, the results for Nu_m are correlated as a function of Gz and are described by the following equations:

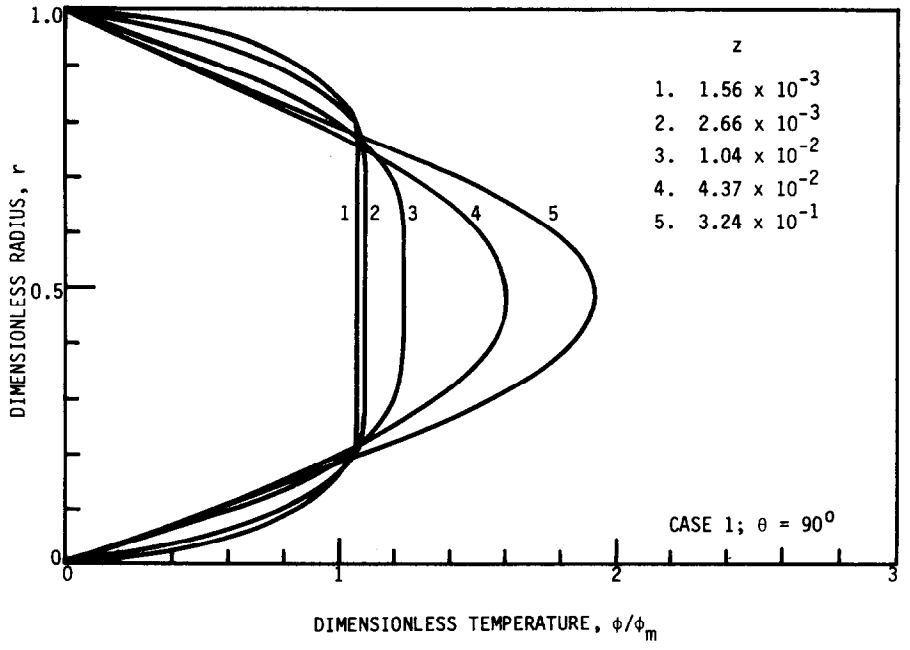

FIG. 6. Development of the temperature profile in the entrance region of the semi-circular duct with Case 1 boundary condition.

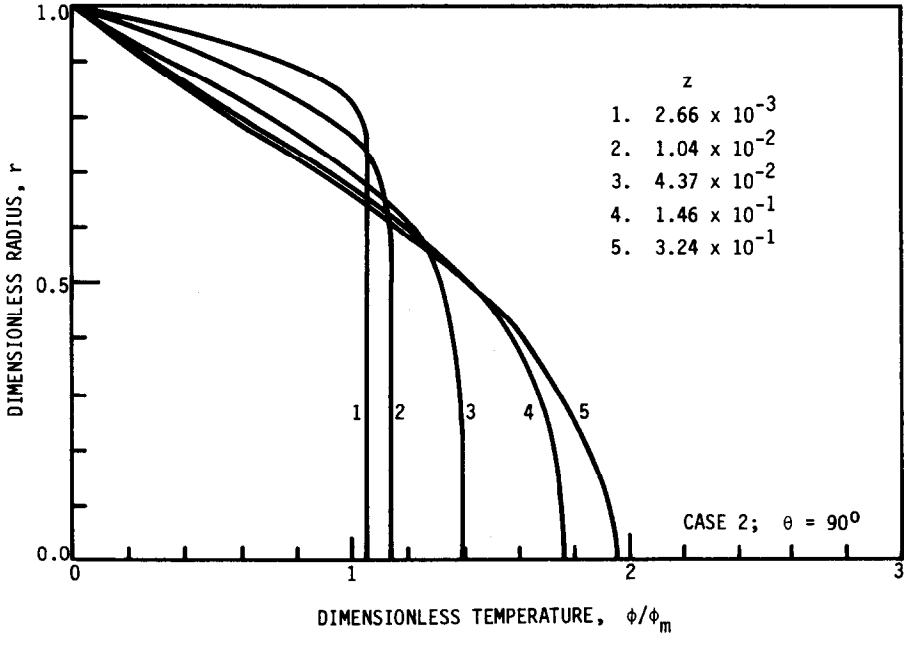

FIG. 7. Development of the temperature profile in the entrance region of the semi-circular duct with Case 2 boundary condition.

Case 1

$$Nu_m = 5.626[1+0.0533(Gz)^{0.9614}]^{1/2.1}; \quad (28)$$

Case 2

$$Nu_m = 4.631[1+0.0954(Gz)^{0.8685}]^{1/1.9}. \quad (29)$$

These equations predict the numerical data within $\pm 2.5\%$.

A comparative presentation of the heat transfer results of the two cases along with the UWT solution for circular tubes [2] is given in Fig. 10. As would be expected, the Nusselt numbers for the two cases seem close in the entrance region and diverge somewhere downstream as the fully developed condition is attained. The larger heat transfer area of the Case 1

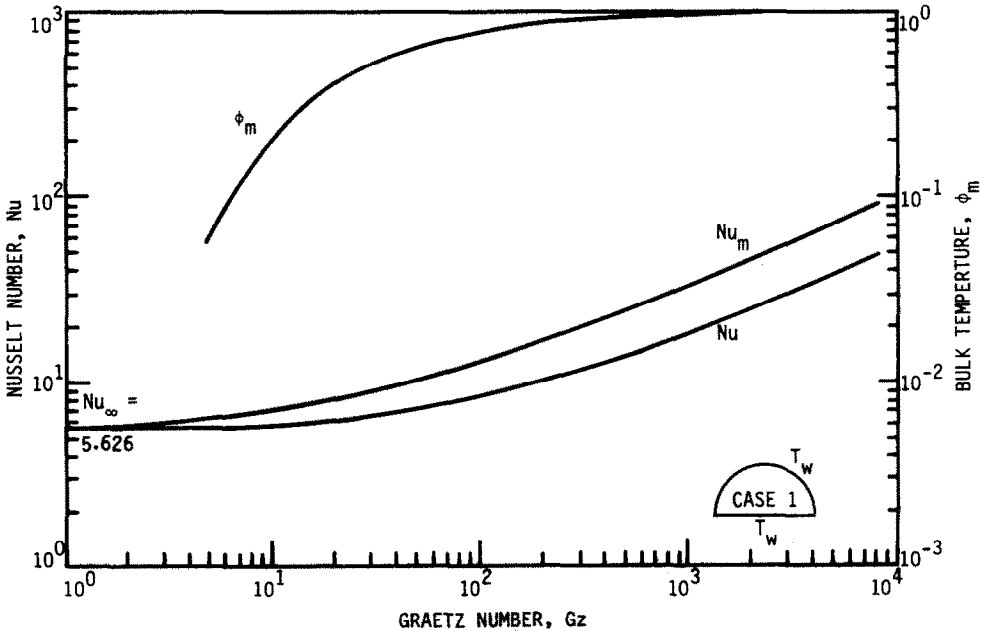

FIG. 8. Thermally developing flow heat transfer results for semi-circular tubes with Case 1 boundary condition.

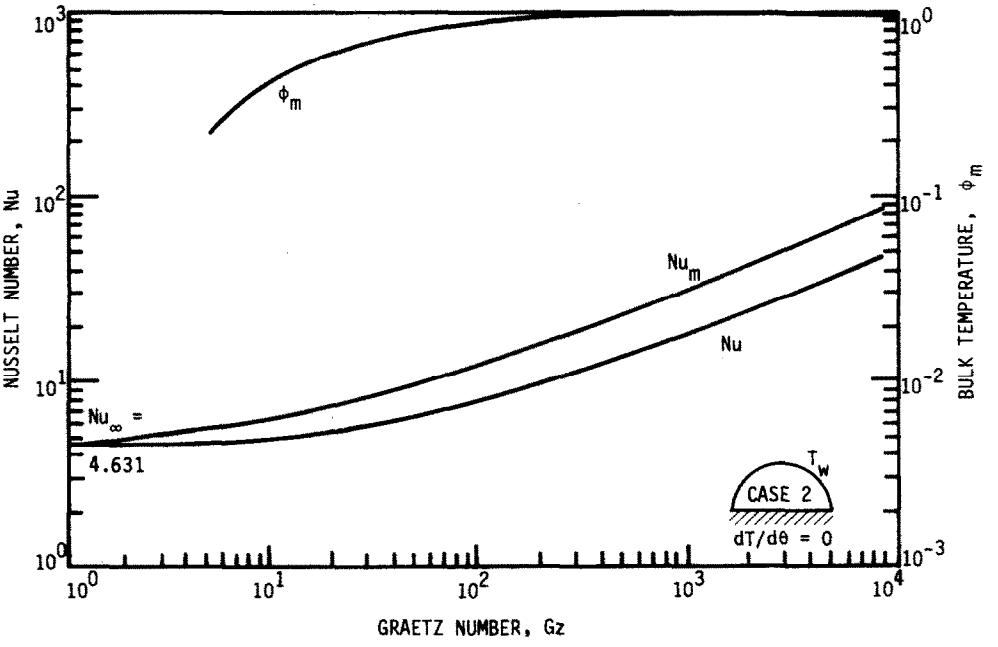

FIG. 9. Thermally developing flow heat transfer results for semi-circular tubes with Case 2 boundary condition.

thermal boundary condition is reflected in higher heat transfer coefficients in comparison with those for Case 2. Nonetheless, the Nusselt numbers for both cases are higher than the corresponding values for a circular tube.

CONCLUSIONS

A numerical solution for constant property, laminar flow in a semi-circular tube with UWT was carried out. The semi-circular tube idealizes the geometry for

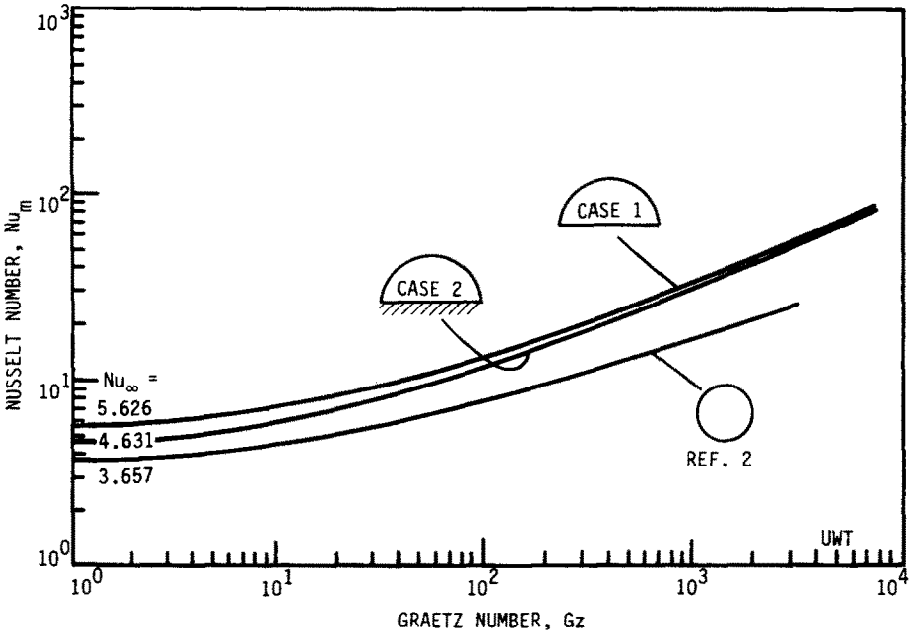

FIG. 10. Heat transfer results in the thermal entrance region of semi-circular and circular tubes with UWT (see also equations (28) and (29)).

an infinite twist ratio, zero thickness strip insert in a circular duct. Heat transfer in both the thermal entrance region and fully developed region was considered. The flow was taken to be hydrodynamically fully developed. Two thermal boundary conditions, described by Case 1 and Case 2 and corresponding to the two extremes of the fin effect of the twisted tape, were chosen. The friction factor was determined to be $(15.823/Re)_{D_h}$, which is in excellent agreement with the published analytical result [4]. The thermal entrance region heat transfer results for the Case 1 and Case 2 boundary conditions are given and the asymptotic Nusselt numbers are 5.626 and 4.6341, respectively. The Nu_m results for the two cases were also formulated into predictive equations as given by equations (28) and (29).

These solutions define the limiting condition of the fin effect of a twisted-strip insert in a circular tube [11]. The Case 2 solution of equation (29), in particular, provides the theoretical lower limit reference for the correlation of experimental data [17] and the interpretation of the heat transfer enhancement phenomenon in circular tubes with twisted-strip inserts.

Acknowledgements—This study was supported by Brown Fintube Co., Houston, Texas, and carried out in the Heat Transfer Laboratory of the Department of Mechanical Engineering, Iowa State University, Ames, Iowa. The advice and assistance of Prof. R. H. Pletcher, Prof. J. M. Prusa, and Mr I.-T. Chiu are much appreciated.

REFERENCES

1. A. E. Bergles and S. D. Joshi, Augmentation techniques for low Reynolds number in-tube flow. In *Low Reynolds Number Flow Heat Exchangers* (Edited by S. Kakaç, R. K. Shah and A. E. Bergles), pp. 695–720. Hemisphere, Washington, D.C. (1983).
2. R. K. Shah and A. L. London, *Laminar Flow Forced Convection in Ducts*, Supplement 1 to *Advances in Heat Transfer*. Academic Press, New York (1978).
3. E. R. G. Eckert, T. F. Irvine, Jr. and J. T. Yen, Local laminar heat transfer in wedge-shaped passages, *Trans. Am. Soc. Mech. Engrs* **80,** 1433–1438 (1958).
4. E. M. Sparrow and A. Haji-Sheikh, Flow and heat transfer in ducts of arbitrary shape with arbitrary thermal boundary conditions, *J. Heat Transfer* **88,** 351–358 (1966).
5. S. W. Hong and A. E. Bergles, Laminar flow heat transfer in the entrance region of semi-circular tubes with uniform heat flux, *Int. J. Heat Mass Transfer* **19,** 123–124 (1976).
6. W. M. Kays and M. E. Crawford, *Convective Heat and Mass Transfer*, 2nd Edn. McGraw-Hill, New York (1980).
7. S. N. Singh, Heat transfer by laminar flow in a cylindrical tube, *Appl. Scient. Res.* **A7,** 325–340 (1958).
8. M. W. Collins, Viscous dissipation effects on developing laminar flow in adiabatic and heated tubes, *Proc. Instn Mech. Engrs* **189,** 129–137 (1975).
9. A. E. Bergles, Prediction of the effects of temperature-dependent fluid properties on laminar heat transfer. In *Low Reynolds Number Flow Heat Exchangers* (Edited by S. Kakaç, R. K. Shah and A. E. Bergles), pp. 451–471. Hemisphere, Washington, D.C. (1983).
10. A. E. Bergles, Experimental verification of analyses and correlation of the effects of temperature-dependent fluid properties on laminar heat transfer. In *Low Reynolds Number Flow Heat Exchangers* (Edited by S. Kakaç, R. K. Shah and A. E. Bergles), pp. 473–486. Hemisphere, Washington, D.C. (1983).
11. R. M. Manglik and A. E. Bergles, An analysis of laminar flow heat transfer in uniform wall temperature circular tubes with tape inserts, Heat Transfer Laboratory Report HTL-39, ISU-ERI-Ames-86290, Iowa State University, Ames, Iowa (May 1986).
12. R. W. Hornbeck, Numerical marching techniques for fluid flows with heat transfer, NASA SP-297, National

Aeronautics and Space Administration, Washington, D.C. (1973).
13. D. A. Anderson, J. C. Tannehill and R. H. Pletcher, *Computational Fluid Mechanics and Heat Transfer*. Hemisphere, Washington, D.C. (1984).
14. N. Conley, A. Lawal and A. S. Mujumdar, An assessment of the accuracy of numerical solutions to the Graetz problem, *Int. Commun. Heat Mass Transfer* **12**, 209–218 (1985).
15. M. W. Collins, Finite difference analysis for developing laminar flow in circular tubes applied to forced and combined convection, *Int. J. Numer. Meth. Engng* **15**, 381–404 (1980).
16. S. W. Hong and A. E. Bergles, Augmentation of laminar flow heat transfer in tubes by means of twisted-tape inserts, Heat Transfer Laboratory Report HTL-5, ISU-ERI-Ames-75011, Iowa State University, Ames, Iowa (December 1974).
17. R. M. Manglik and A. E. Bergles, A correlation for laminar flow enhanced heat transfer in uniform wall temperature circular tubes with twisted-tape inserts, to be presented at the 1987 National Heat Transfer Conference, Pittsburgh, Pennsylvania (August 1987).

CONVECTION THERMIQUE LAMINAIRE DANS UN TUBE SEMI-CIRCULAIRE AVEC TEMPERATURE PARIETALE UNIFORME

Résumé—On analyse la convection thermique laminaire dans un tube semi-circulaire avec paroi à température uniforme, les propriétés du fluide étant constantes. Les résultats définissent la limite inférieure de l'augmentation du transfert de chaleur dans les tubes circulaires avec des inserts à bandes vrillées. On considère deux conditions aux limites thermiques correspondant à deux extrêmes pour l'effet d'ailette des inserts que l'on rencontre dans les applications pratiques. Des solutions numériques employant les formulations de différences finies ont été développées. Pour un écoulement hydrodynamiquement établi, le coefficient de frottement égal à $(15{,}823/Re)_{D_h}$ s'accorde avec la solution analytique trouvée dans la bibliographie. Des résultats pour le transfert thermique en zone d'établissement sont présentés graphiquement et les équations (28) et (49) décrivent les solutions de Nu_m en fonction de Gz pour les deux conditions aux limites. Les nombres de Nusselt asymptotiques sont 5,626 et 4,631 pour les deux cas.

WÄRMEÜBERTRAGUNG IN LAMINARER STRÖMUNG IN EINEM HALBKREISFÖRMIGEN ROHR MIT EINHEITLICHER WANDTEMPERATUR

Zusammenfassung—Der Wärmeübergang in laminarer Strömung in einem halbkreisförmigen Rohr wurde für einheitliche Wandtemperatur und konstante Stoffeigenschaften analysiert. Die Ergebnisse definieren die untere Grenze für die Verbesserung des Wärmeübergangs in kreisrunden Rohren mit Einbauten aus verdrillten Bändern. Dabei werden zwei thermische Randbedingungen betrachtet, die den beiden Extremen des Rippeneffekts entsprechen, welchen man in der praktischen Anwendung begegnet. Es wurden numerische Lösungen mit Hilfe eines Finite-Differenzen-Verfahrens ermittelt. Für eine hydrodynamisch voll ausgebildete Strömung stimmt der Reibungsfaktor von $(15{,}823/Re)_{D_h}$ mit der analytischen Lösung aus der Literatur überein. Ergebnisse für die Wärmeübertragung in der thermischen Einlaufstrecke sind grafisch dargestellt. Die Gleichungen (28) und (29) beschreiben die Nu-Zahl als Funktion der Gz-Zahl für die beiden Randbedingungen. Die asymptotischen Nusselt-Zahlen für die beiden Fälle sind 5,626 bzw. 4,631.

ТЕПЛОПЕРЕНОС ПРИ ЛАМИНАРНОМ ТЕЧЕНИИ В ПОЛУКРУГЛОЙ ТРУБЕ С РАВНОМЕРНО НАГРЕТОЙ СТЕНКОЙ

Аннотация—Анализируется теплоперенос при ламинарном течении жидкости с постоянными свойствами в полукруглой трубе с равномерно нагретой стенкой. Результаты позволяют определить нижний предел интенсификации теплообмена в круглых трубах с извилистыми ленточными вставками. Рассмотрено два вида тепловых граничных условий, соответствующих двум встречающимся на практике предельным случаям влияния ребер вставок. Получены численные решения с использованием конечно-разностных формулировок. Для гидродинамически полностью развитого течения коэффициент трения, равный $(15{,}823/Re)_{D_h}$, согласуется с известным значением, рассчитанным аналитически. Результаты по теплообмену при термически неустановившемся течении представлены графически. Уравнения (28) и (29) дают решения для зависимости числа Nu_m от Gz для двух граничных условий. Асимптотические значения числа Нуссельта для этих двух случаев равны 5,626 и 4,631.